

Audio-Visual Target Speaker Extraction with Reverse Selective Auditory Attention

Ruijie Tao, Xinyuan Qian, *Senior Member, IEEE*, Yidi Jiang, Junjie Li, Jiadong Wang and Haizhou Li, *Fellow, IEEE*

Abstract—Audio-visual target speaker extraction (AV-TSE) aims to extract the specific person’s speech from the audio mixture given auxiliary visual cues. Previous methods usually search for the target voice through speech-lip synchronization. However, this strategy mainly focuses on the existence of target speech, while ignoring the variations of the noise characteristics. That may result in extracting noisy signals from the incorrect sound source in challenging acoustic situations. To this end, we propose a novel reverse selective auditory attention mechanism, which can suppress interference speakers and non-speech signals to avoid incorrect speaker extraction. By estimating and utilizing the undesired noisy signal through this mechanism, we design an AV-TSE framework named Subtraction-and-Extraction network (SEANet) to suppress the noisy signals. We conduct abundant experiments by re-implementing three popular AV-TSE methods as the baselines and involving nine metrics for evaluation. The experimental results show that our proposed SEANet achieves state-of-the-art results and performs well for all five datasets. We will release the codes, the models and data logs.

I. INTRODUCTION

THE human brain is capable of selectively listening to a specific voice and filtering out other sounds in situations where there are multiple talkers and non-speech noises. This phenomenon is known as the ‘selective auditory attention’ [1]–[3]. Inspired by that, the audio-visual target speaker extraction (AV-TSE) task has been studied to mimic this ability. In AV-TSE, neural networks can comprehend the lip movements of the target speaker and extract the corresponding clean speech [4] from the heard mixture of audio. In practice, AV-TSE does not require prior knowledge of the speaker amount [5], [6] and relies on synchronized facial expressions to focus on the target speaker’s voice only. As an essential front-end, AV-TSE can assist various downstream multi-modal tasks such as audio-visual speech recognition [7], [8], speaker diarization [9], [10] and recognition [11], [12]. It can also

Ruijie Tao, Yidi Jiang and Jiadong Wang are with the Department of Electrical and Computer Engineering, National University of Singapore, Singapore (e-mail: ruijie.tao@u.nus.edu, yidi_jiang@u.nus.edu and jiadong.wang@u.nus.edu) (*Corresponding author: Jiadong Wang*).

Xinyuan Qian is with the Department of Computer Science and Technology, University of Science and Technology Beijing, Beijing, 100083, China. (email: qianxy@ustb.edu.cn)

Junjie Li is with the Chinese University of Hong Kong (Shenzhen), 518172 China (e-mail: mrjunjieli@gmail.com).

Haizhou Li is with the Guangdong Provincial Key Laboratory of Big Data Computing, the Chinese University of Hong Kong (Shenzhen), 518172 China; also with Shenzhen Research Institute of Big data, Shenzhen, 518172 China; also with the Department of Electrical and Computer Engineering, National University of Singapore, 119077, Singapore and also with the University of Bremen, 28359 Germany. (e-mail: haizhouli@cuhk.edu.cn)

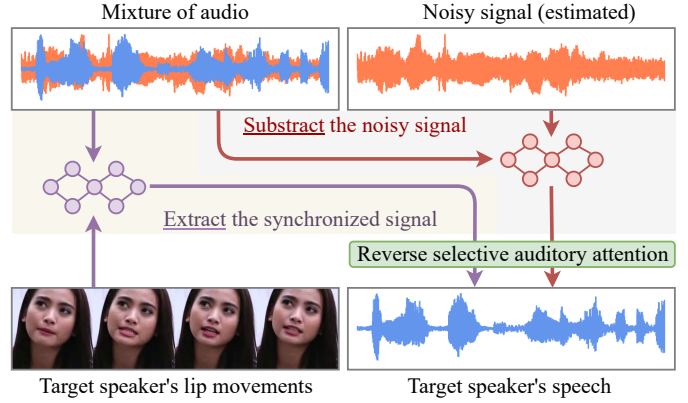


Fig. 1. Typical approaches in AV-TSE focus on ‘Extraction’, which searches for the target speaker’s voice from the audio mixture to match the corresponding lip movements. However, the extraction results may involve noisy signals from incorrect sound sources. To alleviate these problems, we introduce the complementary ‘subtraction’ strategy. By analyzing the reverse selective auditory attention, our proposed method utilizes the estimated noisy signal and excludes them during extraction.

be applied to augmented reality (AR) glasses and robots to improve the quality of the heard voice [13].

The foundation of AV-TSE lies in the synchronization between lip movements and speech waveform [14], [15]. In an audio mixture, the target speech inside represents the pronunciation of phonemes, while the lip movements of the target speaker correspond to the viseme signals [16], [17]¹. By establishing a temporal correlation between visemes and the corresponding speech signal components, it becomes possible to associate and align these two different modal signals [18]. Following this principle, an efficient AV-TSE solution is to encode visual lip frames into the embedding sequence, and feed it into the extractor module for obtaining the clean speech waveform. In particular, different architectures have been studied, such as convolutional neural networks (CNN) [4], [19], [20], temporal convolutional networks (TCN) [5], [14], [21], [22], cross-modal transformer [6], [23] and dual-path recurrent neural network networks (DPRNN) [24], [25].

As depicted in the left part of Figure 1, most existing AV-TSE methods only focus on the ‘extraction’ strategy to search for the speech waveform component that is time-aligned with lip movements [4]–[6]. However, due to the generalization ability of the neural network, the extracted speech with a

¹Viseme represents a basic visual speech unit that links to the phoneme of acoustic speech.

proper range of noise can also be considered synchronized with the lip movement by the model. So these methods may inadvertently involve noisy signals or even separate some voices from the wrong source [26]. That inspires us to guide the model in perceiving noisy signals during extraction. Additionally, some studies in image denoising and speech recognition have revealed the significance of investigating noisy signals as the auxiliary [27]–[29]. These findings motivate us to design a dedicated module that explicitly fits the AV-TSE task for exploring the speech-noise mutual exclusivity, i.e., reverse selective auditory attention. We summarise that as the ‘*subtraction*’ strategy (as indicated by the right part of Figure 1), which aims to estimate and understand the noisy signal in AV-TSE to improve training efficiency and system performance.

In this paper, we propose a reverse attention mechanism to exclude the noisy information in AV-TSE to achieve this mutual exclusivity. It takes the target speech and the noisy signal for frame-level cross-attention. Suppose two audio frames from the respective signal achieve a high correlation score, these components should be penalized for incorrect extraction. This design can remove undesirable audio and avoid incorrect speaker extraction. Meanwhile, considering that noise includes interference speakers and background audio, which are all out-of-sync with the target speaker’s lip movements, we design a parallel speech and noise learning (PSNL) block to estimate speech and noisy signals at the same time. By inserting the reverse attention mechanism into the PSNL block, the model can perceive the noisy signal during the extraction process by combining the ‘*extraction*’ and ‘*subtraction*’ strategies.

The contributions in this paper can be listed as:

- 1) To avoid the presence of noisy information and incorrect speech in audio-visual target speaker extraction, we propose a specific reverse attention module to achieve the mutual exclusivity between the target speaker’s speech and the noisy signal.
- 2) Based on that, we propose the Subtraction-and-ExtrAction network (*SEANet*), a novel AV-TSE system with reverse selective auditory attention to assist the extraction by excluding the noisy signal. *SEANet* contains the PSNL block to estimate the speech and noisy signal.
- 3) We conduct the results on five datasets for in-domain and cross-domain evaluation. With solid comparison by re-implementing three baseline methods, *SEANet* achieves state-of-the-art results for all nine metrics.

II. RELATED WORK

A. Target speaker extraction

In social activity scenarios, the auditory environment often comprises a complex mixture of several speakers’ voices with reverberation and background noise [30], [31]. Traditional speech separation (SS) aims to estimate the individual speech sources of each speaker from the mixture signal directly [24], [32], [33]. It struggles with assigning separated speech to the correct speakers [34]. Inspired by human perception [35], target speaker extraction (TSE) treats the person of interest as the target speaker to imitate selective auditory attention ability:

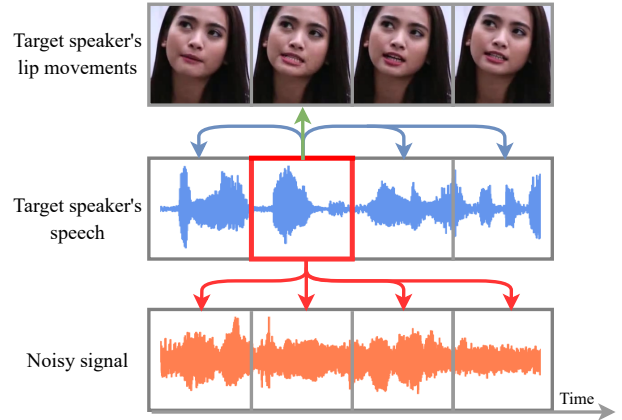


Fig. 2. Available auxiliary references in AV-TSE. Green line: speech-lip synchronization (positive correlated); Blue line: voice consistency (positive correlated); Orange line: speech-noise exclusivity (negative correlated).

In TSE, An auxiliary reference from the target speaker is provided to direct the target person. By leveraging this reference, the neural network can effectively extract the target speaker’s voice from the audio mixture [5], [36], [37]. TSE does not require prior information of the total speaker number [35]. Meanwhile, benefits from the reference signal to supervise the extraction, TSE can prevent unreliable blind source separation.

B. Auxiliary references in target speaker extraction

1) *Pre-enrolled speech*: The widely-used auxiliary reference is the target speaker’s pre-enrolled speech utterance [36], [37]. Each speaker possesses the distinctive voice characteristics, which can be modelled into a fixed dimensional vector, referred to as the speaker embedding [38]–[40]. Previous works [30], [35], [41] have employed the speaker encoder to derive speaker embedding from the reference speech, subsequently serving as attractors in the extraction process [42], [43]. Inspired by that, we propose to leverage the inherent consistency of the target speaker’s voice for AV-TSE. As illustrated by the blue lines in Figure 2, we expect that each frame of the extracted speech exhibits a high degree of correlation with the others due to the consistent voiceprint.

2) *Speech-lip synchronization*: The facial information, particularly the lip movements of the target speaker, can be used as the auxiliary reference in extraction through speech-lip synchronicity [4]. Following this idea, several AV-TSE algorithms have been proposed, such as MuSE for self-enrollment [5], USEV for sparse overlap scenario [25] and TDSE for time-domain modeling [14]. These methods use a visual encoder to learn lip embedding sequences of the target speaker, which are then temporally aligned with speech frames. As shown by the green lines in Figure 2, during extraction, the interaction occurs between the concurrent speech frames and the visual lip frames [15], [20], [44].

3) *Speech-noise exclusivity*: Noise always comes with speech, this correlation (speech-noise exclusivity) can provide complementary guidance for extraction. For example, in computer vision, extracting noise from images can contribute

to the denoising process [45]; In speech recognition and enhancement, the consideration of noise can improve the system through a lightweight interaction layer [28], [29]. These findings demonstrate the importance of involving noise exploration. However, as illustrated by the red lines in Figure 2, this inter-frame mutual exclusivity between the target speaker’s speech and the noisy signal (refer as the ‘reverse selective auditory attention’ mechanism) has not been explored in AV-TSE. Meanwhile, previous studies in object detection and polyp segmentation [27], [46] studied the concept of reverse attention, which eliminates the core regions to make the model focus on local details. Inspired by that and modified based on the standard self-attention mechanism, we propose the reverse attention module. It penalizes segments with high speech-noise consistency since they should be mutually exclusive.

III. SEANET

A. Task formulation and data generation

We define x as a mixture of audio in the time domain, which contains the target speaker’s voice s , the interference speaker’s voice o_i and the background non-speech signal b :

$$x = s + \sum_{i=1}^N o_i + b \quad (1)$$

where N is the number of interference speakers that ≥ 1 . Given the visual frames of the target speaker, which are denoted as v , AV-TSE aims to obtain \hat{s} to approximate s . v and s should be synchronized.

As shown in Figure 3, in data generation process, we sum the speech from other speakers and the non-speech signal to generate the noisy signal: $n = \sum_{i=1}^N o_i + b$. Then x can be obtained by summing n and s . In our proposed SEANet, v and x are fed as the inputs which are encoded into the visual and audio embeddings to be fused and segmented into the multimodal embedding. In order to obtain the embedding of the target speaker’s speech and the noisy signal for the subsequent interaction, the pre-extractor and pre-suppressor modules are designed. Then several parallel speech and noise learning (PSNL) blocks are serially connected to learn the reverse selective auditory attention. Each PSNL block contains the reverse attention module to penalize the incorrect extraction. Finally, the embedding of the target speaker’s speech and the noisy signal are aggregated and decoded into the estimated target speaker’s speech \hat{s} and the estimated noisy signal \hat{n} . Note that only \hat{s} is required during evaluation.

B. Audio and visual encoder

For audio input, the mixture of input audio x is the 1-dimensional (1D) signal in the time domain with the length of T . The audio encoder is viewed as a frequency analyzer to output the 2D frame-based embedding sequence $X \in R^{D_a \times L}$. This encoder consists of a 1D-CNN and a rectified linear activation (ReLU). D_a and L is the audio embedding dimension and the number of audio frames, respectively. The duration of each audio frame is decided by 1D CNN’s stride size.

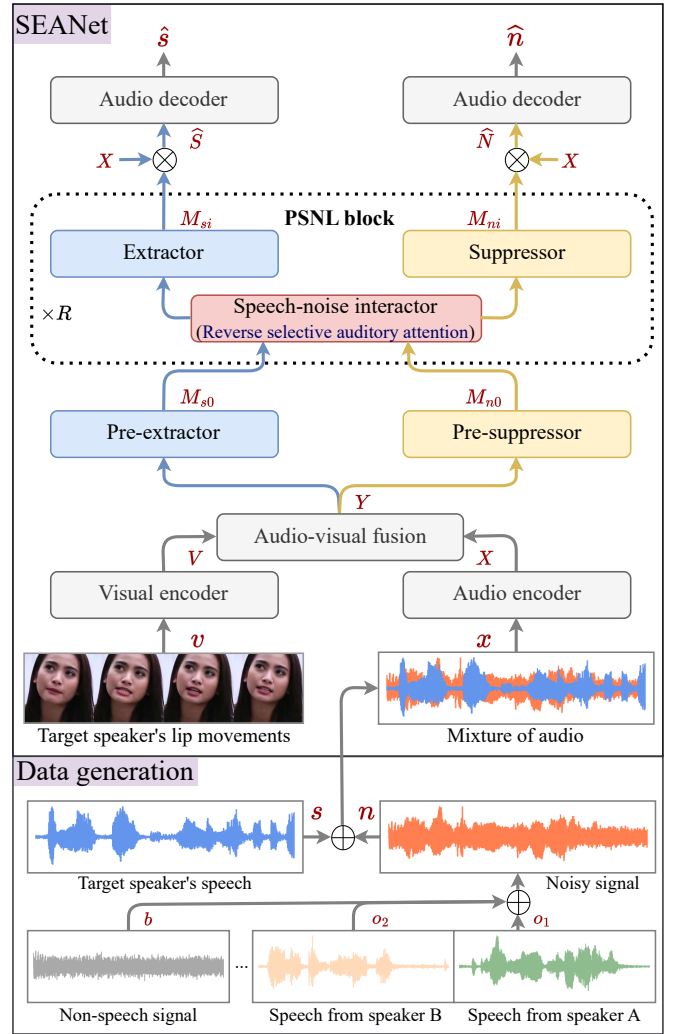


Fig. 3. The bottom panel is the data generation process for AV-TSE, the upper panel is our proposed SEANet. It extracts the clean speech of the target speaker from the mixture of audio. Specifically, SEANet contains R repeated PSNL blocks to learn the reverse selective auditory attention between the estimated clean speech and noisy signal, M_{si} and M_{ni} are the output speech and noise embeddings from the i^{th} block, respectively. \oplus represents entrywise sum (to mix up audios) and \otimes represents matmul product. Note that Pre-extractor and Pre-suppressor share the same model architecture with Extractor and Suppressor, respectively.

For visual inputs, a CNN-based visual encoder is utilized to discern lip movements from static face frames, with a focus on the specific mouth shape. The target speaker’s face frames v are processed, where a central crop is applied to isolate and efficiently represent the lip region. The visual frame representations are generated using a 3D-CNN layer followed by a ResNet18 block, as detailed in [47]. Subsequently, the Video Temporal Convolutional block (V-TCN) is engaged to extract temporal dynamics of lip movements and to identify the corresponding viseme. This V-TCN comprises a sequence of five residual connections, each integrating a Rectified Linear Unit (ReLU), batch normalization (BN), and a depth-wise separable convolutional layer (DS-Conv1D), as outlined in [14]. The output embedding is then up-sampled to $V \in R^{D_v \times L}$, aligning with the temporal resolution of the audio embedding X (D_v denotes the embedding dimension).

C. Audio-visual fusion

Previous research has confirmed that temporally aligning and concatenating audio and visual features is an effective approach for feature extraction [5], [14]. Based on that, the audio embedding X is passed through a group normalization (GN) and a 1D-CNN layer. Subsequently, X is concatenated with V along the temporal dimension, which is then further refined by an additional 1D-CNN layer. The dimension of the integrated audio-visual embedding is $R^{D \times L}$ where D represents the embedding dimension.

To manage long feature sequences of variable lengths, the segmentation operation effectively divides the audio-visual embedding into multiple, overlapping segments along the temporal axis, as described in [24]. The segmentation utilizes a window size of K and a hop size of $K/2$, yielding P segments, which are concatenated to create a 3D tensor $Y \in R^{D \times K \times P}$. After we obtain the embedding of the clean target speech M_{si} (which will be introduced later), an aggregation step, acting as the inverse of segmentation, reconstitutes the 3D tensor into a 2D tensor. It undergoes a parametric rectified linear unit (pReLU) activation and passes through a 1D-convolutional (1D-Conv) layer to derive the estimated speech embedding \hat{S} . A parallel process is employed to attain the estimated noisy embedding \hat{N} . Noted that the segmentation and aggregation processes are not explicitly illustrated in Figure 3.

D. Pre-extractor and pre-suppressor

To achieve the subsequent speech-noise interaction process, we initially estimate the embeddings of the target speaker’s speech and the accompanying noise. As depicted in Figure 3, the audio-visual embedding Y is fed into the pre-extractor and pre-suppressor to obtain the initial embedding M_{s0} for the target speech and M_{n0} for the noisy signal, respectively. These pre-processing modules are adaptations of DPRNN [24]. Note that the extractor and suppressor (which are elaborated in the subsequent PSNL section) share identical model architectures with their pre-processing counterparts. The details have been illustrated in Figure 4.

Pre-extractor contains an intra-chuck module followed by an inter-chuck module. In the intra-chuck module, a Bidirectional Long Short-Term Memory (BLSTM) layer is applied to integrate the knowledge within each chunk. The length of each chunk, denoted as K , is considered as the sequence length for the BLSTM. This BLSTM is followed by a linear layer with GN. The inter-chuck module has a similar network structure. The difference is that the sequence length in BLSTM is the number of chunks P . This enables the knowledge integration across the different chunks.

Pre-suppressor is designed to estimate the embedding of the noisy signal. It has the same model structure as the extractor to search for the out-of-sync audio signal with the visual frames. This suppressor works in parallel with the extractor.

E. Parallel speech and noise learning (PSNL)

After that, parallel speech and noise learning (PSNL) block is used to learn the reverse selective auditory attention. M_{s0}

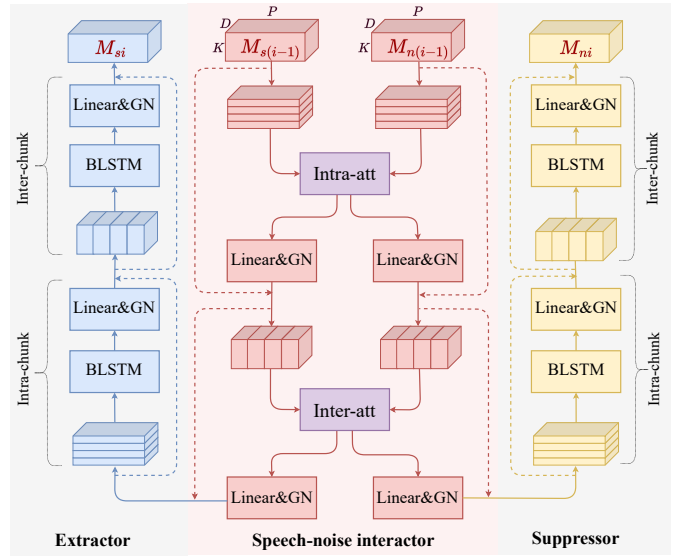


Fig. 4. The i^{th} parallel speech and noise learning (PSNL) block. Intra-att and Inter-att blocks are used to learn the interaction between the target speaker’s speech and the noisy signal. M_{si} and M_{ni} are the output embeddings of the speech and the noise, respectively. Dash lines denote residual connections. Pre-extractor/suppressor in Fig 3 has the same structure as the extractor/suppressor, while the input is Y , and the output is M_{s0} or M_{n0} .

and M_{n0} are fed into R PSNL blocks. These blocks have non-shared parameter weights and are serially connected. In the i^{th} PSNL block, the inputs are the speech embedding $M_{s(i-1)}$ and the noise embedding $M_{n(i-1)}$ from the $(i-1)^{th}$ PSNL block ($i \in [1, R]$). First, the intra-chuck attention (intra-att) module is used to learn the speech-noise mutual exclusivity within each chunk, which can avoid incorrect extraction in local frames. The output embeddings go through the linear layers with GN operation. Then, with a similar structure, an inter-att module is applied to compare the speech and noisy signals from different chunks to learn the global correctness. Here, the length of each chunk K and the number of chunks P are viewed as the sequence length in the intra-att and inter-att module, respectively. As shown in Figure 4, after the speech-noise interactor, an extractor and a suppressor are used to optimize the embedding of the target speaker’s speech and the noisy signal. This extractor (suppressor) have the same model architecture to the pre-extractor (pre-suppressor).

F. Reverse attention module

Figure 5 explains the details of the intra-att and inter-att module. They have the similar structure, and each integrating a self-attention component and a reverse attention component. Specifically, the self-attention mechanism assigns higher weights to audio frames that exhibit a strong correlation to enhance the voice consistency. Conversely, the reverse attention mechanism conducts a frame-level cross-attention analysis between the target speech signal and the accompanying noise. If two audio frames from the respective signal achieve a high correlation score, that represents the extracted speech segment is similar to the estimated noisy signal. In other words, the extracted speech may contain noise and should be penalized.

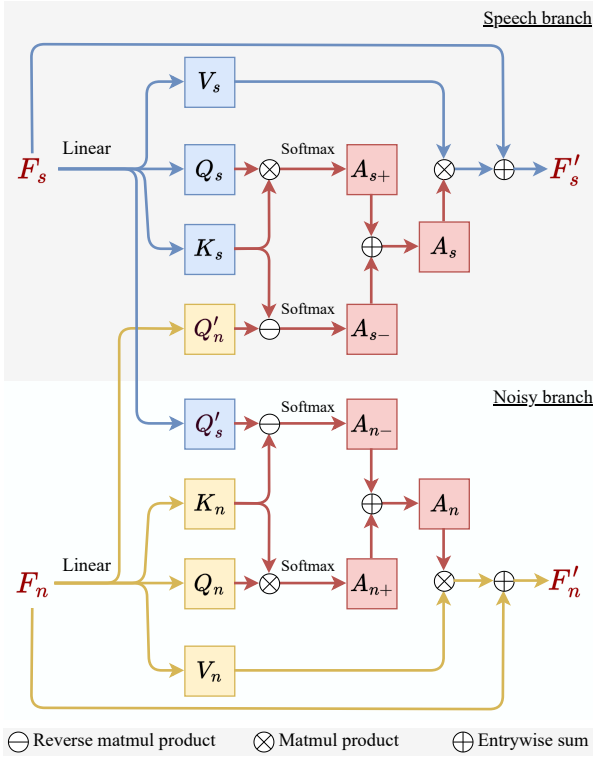


Fig. 5. Illustration of the intra-chunk attention module (intra-att) or the inter-chunk attention module (inter-att). F_s and F_n represent the input speech and noisy embedding, respectively. F'_s and F'_n denote their respective processing outputs. This module contains the self-attention score A_{s+} to learn the speechlip relationship and the reverse attention score A_{s-} to comprehend the speech-noise mutual exclusivity.

We designate the inputs to the intra-chunk attention module as F_s , representing the 3D speech embedding, and F_n , representing the noise embedding. Four linear layers are used for the speech branch to obtain V_s , Q_s , K_s and Q'_s . Here, Q_s serves as the query vector in self-attention to ensure voice consistency. Q'_s operates as the query vector in reverse attention for speech-noise exclusivity. K_s and V_s are the key and value of speech, respectively. With a similar approach, V_n , Q_n , K_n and Q'_n can be obtained from the noise embedding F_n .

For self-attention, the extracted speech segments should exhibit consistent voice characteristics across the temporal dimension. To this end, we multiply the query and key from speech to get the attention matrix A_{s+} . This matrix awards the extracted segment if it shares a consistent voice representation in an utterance.

For reverse attention, the extracted speech should exclude the interference signal with low correlation: After multiplying the speech key and the noisy query, the output attention matrix goes through a reverse operation for the opposite attention matrix A_{s-} . Based on that, the high-corrected parts will be transferred into a low negative score to represent the incorrect extraction. The subsequent softmax operation $\sigma(\cdot)$ can ensure the final score matrix is in an appropriate range. The final score matrix A_s is defined as:

$$A_s = \frac{1}{2} \left(\underbrace{\sigma\left(\frac{Q_s \cdot K_s^T}{\sqrt{D}}\right)}_{A_{s+}} + \underbrace{\sigma\left(-\frac{Q'_n \cdot K_s^T}{\sqrt{D}}\right)}_{A_{s-}} \right) \quad (2)$$

which is the average of the self-attention score A_{s+} and reverse attention score A_{s-} to judge the quality of each extracted speech segment. It is then multiplied with the value of speech, followed by the residual connection to get the output embedding F'_s .

$$F'_s = A_s \cdot V_s + F_s \quad (3)$$

As described in Figure 5, the noisy branch has the symmetrical structure to obtain the F'_n . Meanwhile, intra-att and inter-att share the similar structure, the difference is that the size of score matrix is $K \times K$ in intra-att and $P \times P$ in inter-att, respectively.

G. Audio decoder and constraints design

The final output embeddings are represented as M_{sR} and M_{nR} . They are element-wise multiplied with X , respectively, followed by two audio decoder (shared weights) to obtain the estimated temporal target speech $\hat{s}_R \in R^{1 \times T}$ and noisy signal $\hat{n}_R \in R^{1 \times T}$. This decoder comprises a linear layer and an overlap-and-add (OnA) operation from signal processing.

We also multiply M_{si} (and M_{ni}) with X when $i \in [0, R-1]$, followed by the same audio decoder to obtain the speech signal \hat{s}_i (and noisy signal \hat{n}_i) in each PSNL block. They will be involved in training loss to ensure that M_{si} and M_{ni} are direct to speech and noisy information, respectively, to guarantee meaningful speech-noise interaction. We use \hat{s}_R (estimated target speaker's speech from the last PSNL block) to compute the metrics during evaluation.

H. Loss function

The scale-invariant signal-to-distortion ratio (SI-SDR) loss [48] can measure the reconstruction error between the estimated audio \hat{p} and the ground-truth audio p . We denote it by $l(\cdot, \cdot)$:

$$l(\hat{p}, p) = -10 \log_{10} \left(\frac{\|\langle \hat{p}, p \rangle\|^2}{\|\hat{p} - \frac{\langle \hat{p}, p \rangle}{\|p\|^2} p\|^2} \right) \quad (4)$$

Our training loss includes a main loss and an auxiliary loss. The main loss is the SI-SDR loss between the estimated target speaker's speech from the last PSNL block \hat{s}_R and the ground-truth speech s :

$$\mathcal{L}_{main} = l(\hat{s}_R, s) \quad (5)$$

The auxiliary loss considers the outputs from the rest of the extractors and suppressors. It controls the inputs of interactor for training constraints:

$$\mathcal{L}_{aux} = \sum_{i=0}^{R-1} l(\hat{s}_i, s) + \sum_{i=0}^R l(\hat{n}_i, n) \quad (6)$$

The final training loss is the weighted addition of these two losses. We also carry out experiments to study the robustness of this hyper-parameter β .

$$\mathcal{L} = \mathcal{L}_{main} + \beta \cdot \mathcal{L}_{aux} \quad (7)$$

IV. EXPERIMENTAL SETTING

A. Training set

1) *LRS2*: The LRS2 audio-visual speech recognition dataset [47] is derived from BBC television. Each video clip contains one person’s synchronized audio-visual signal. To simulate one mixed audio, we randomly pick one sample’s speech waveform and visual frames as the target speaker’s clean speech and lip movements, respectively. The audio from one other sample is selected as the interference speech. This interference speech is mixed with the target speech with a random signal-to-noise (SNR) ratio between -10 dB and 10 dB. Similar to the previous studies [5], [6], we generate 20,000, 5,000 and 3,000 mixed audios for training, validation and testing, respectively, with no overlapped speaker. We conduct the experiments with multiple people and the non-speech signal to simulate more diverse real-world scenarios in the quality studies.

2) *VoxCeleb2*: VoxCeleb2 [49] is an audio-visual speaker recognition dataset collected from YouTube interviews, which represents more challenging scenarios such as the unclear side face and the strong noise. The data generation pipeline is the same as in processing LRS2.

For in-domain evaluation, our system is trained on VoxCeleb2 or LRS2 and then evaluated on the corresponding test set.

B. Evaluation Set

For cross-domain evaluation, we train the system on VoxCeleb2 and test it on LRS3 [50], Grid [51] and TCD-TIMIT [52]. During the evaluation, we randomly generate 3,000 speech mixtures in each evaluation dataset with variable lengths with the SNR between -10 dB to 10 dB. The details of these sets are listed as follows:

1) *LRS3*: LRS3 is the audio-visual speech dataset collected from the TED videos. As a large-scale speech recognition dataset, LRS3 contains videos with precise lip movements and clear speech. Furthermore, the audio and visual modalities are strictly synchronized. LRS3 can be used for indoor scenario evaluation of videos in the wild.

2) *Grid*: Grid dataset contains the videos from a controlled studio environment. As the multi-talker speech perception dataset for computational-behavioral studies, it has high-quality audio and video recordings. In each video, one speaker sits in front of the camera and reads the given sentence with a fixed head orientation.

3) *TCD-TIMIT*: TCD-TIMIT dataset also consists of the videos collected from the studio condition for speech recognition. In each video, two cameras with different angles are used to collect data, and the speaker is asked to read the given phonetically rich sentence. Both TCD-TIMIT and Grid can be employed for high-quality studio video evaluation.

C. Implementation details

During training, the initial learning rate is 10^{-3} with a decreasing interval of 3% after every three training epochs. The maximum training epoch is set to 150, and the system

is validated every three epochs. Videos are cut into segments with fixed duration during training (2 seconds in LRS2 and 4 seconds in VoxCeleb2). During the evaluation, the entire videos with the variable lengths are applied.

The visual frame rate and audio sampling rate of all videos are 25fps and 16kHz, respectively. The visual inputs are the middle part of all face frames with the size of 112×112 . That operation can improve training efficiency while keeping lip areas. Following all previous works [4]–[6], [14], the visual encoder is pre-trained by lip reading² and it is frozen in all experiments. K, D_a, D_v, D, R, β are set as 100, 256, 256, 64, 5 and 0.1, respectively. Our SEANet contains 8.70M parameters.

D. Baseline methods

To verify the robustness of our SEANet, we involve and re-implement three popular audio-visual speaker extraction systems as the baselines for comparison: AV-DPRNN, MuSE and AV-Sepformer. We build these network architectures and train them with the same setting that used for SEANet to achieve fair comparison.

1) *AV-DPRNN*: AV-DPRNN is the audio-visual dual-path RNN-based TSE system. Compared to SEANet in Figure 3, the difference is that there is no suppressor, pre-suppressor and speech-noise interactor in the AV-DPRNN. As shown in Figure 6, it predicts the target speech only so the performance gap can reflect the effect of reverse selective auditory attention. The loss function considers the output of all $(R+1)$ extractors. That setting is equivalent to the architecture of SEANet. AV-DPRNN has 4.12M parameters.

2) *MuSE*: MuSE (MULTI-modal Speaker Extraction network) [5] is the temporal convolutional network-based system that be modified based on AV-ConvTasNet [14]. Considering that the voiceprint of the target speaker can also provide the reference for extraction, MuSE uses a self-enrollment strategy to learn the speaker embedding during the extraction process. The additional classification loss is applied during training to guide the system in understanding the speaker representation. It is trained on VoxCeleb2 for the original paper, and we re-implement the structure and conduct it on VoxCeleb2 and LRS2. Compared with SEANet, MuSE involves the additional speaker embedding information for the target speaker to guide the extraction. It contains 15.01M parameters, much larger than that in SEANet.

3) *AV-Sepformer*: AV-Sepformer [6] (AV-Sep) is the transformer-based multimodal extraction framework motivated by the transformer-based audio-only speech separation system. It introduces the audio-visual interaction to learn the relationship between the audio and visual modality. AV-Sepformer also contains a dual-path structure to understand inter-chunk and intra-chunk knowledge. Also, it was only studied on VoxCeleb2 for the original paper, and we extended the experiments for the LRS2 dataset. Considering that AV-Sepformer has a very large model architecture, for relatively fair comparison and GPU memory consideration, our study slightly reduced the number of layers in AV-Sepformer. However, it still

²https://github.com/smeetsr/deep_avsr

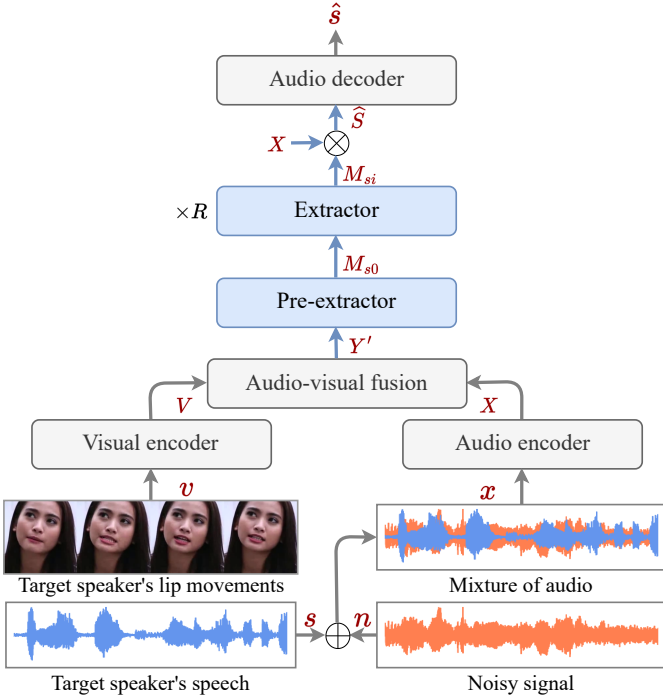


Fig. 6. The AV-DPRNN framework is one of the baseline methods we re-implement. Compared with SEANet, it only contains extractor blocks to focus on the target speaker’s speech.

contains 21.73M parameters, which is around twice than that in SEANet.

E. Metrics

Following the previous works, we use scale-invariant signal-to-distortion ratio (SI-SDR) [48] and signal-to-distortion ratio (SDR) as the main metrics to evaluate the quality of the extracted speech. Their unit is dB. Meanwhile, we introduce several additional metrics to comprehensively judge the quality of the extraction: Perceptual evaluation of speech quality (PESQ) [53] and short-term objective intelligibility (STOI) [54] are introduced to precept the extracted speech. Furthermore, we also report these metrics with the relative improvement (denoted as the suffix ‘*i*’, i.e., $\underline{\text{SI-SDR}}_i$, $\underline{\text{SDR}}_i$, $\underline{\text{PESQ}}_i$ and $\underline{\text{STOI}}_i$). For instance, denote ground-truth speech as s , mixed audio as x , output speech as \hat{s} , there is $\text{SDR}_i = \text{SDR}(\hat{s}, s) - \text{SDR}(x, s)$. Higher is better for these 8 metrics. Moreover, we also compute the word-error-rate (WER) by feeding the extracted speech into the pre-trained automatic speech recognition systems [55]. It can represent the readability and the informativeness of the extracted speech. Lower is better for WER.

V. RESULTS AND ANALYSIS

This section reports the results with five subsections: Section V-A compares SEANet with the baseline methods and other previous methods for in-domain evaluation. Both the results on LRS2 and VoxCeleb2 dataset have been provided. Section V-B reports the cross-domain evaluation result for SEANet and the baseline methods. The evaluation sets are

LRS3, Grid and TCD-TIMIT datasets. In Section V-C, we conduct the ablation study to verify the efficiency of the architecture of SEANet, especially for reverse selective auditory attention. Section V-D employs the quality study to prove the robustness of SEANet with different evaluation conditions and settings. Finally, section V-E provides some visualization results.

A. In-domain evaluation: LRS2 and VoxCeleb2

For in-domain evaluation, we conduct the experiments of SEANet and re-implement three pre-mentioned baselines with the same training setting for comparison. For LRS2 dataset training and evaluation, we report all nine metrics for four methods, for the experiments on the VoxCeleb2 dataset, WER cannot be reported since there is no public text labels. Meanwhile, we also provide the results of other previous methods based on the results in their published paper and compare them with SEANet.

1) Comparison with baseline methods on the LRS2:

Table I contains the results of SEANet and baseline methods for all metrics. All four methods are trained and evaluated on LRS2 with the same setting by our effects. SEANet performs the 13.08 dB SI-SDR and 13.67 dB SDR, which is better than other methods, for instance, 12.60 dB SI-SDR from AV-Sep. SEANet also achieves the best PESQ and STOI (2.25 and 0.92). On the other hand, SEANet achieves better relative improvement on these four metrics. Furthermore, SEANet obtains a lower WER than the other three baseline methods, representing stronger readability. These results prove that our proposed SEANet can perform well for the AV-TSE task with a relatively lightweight model architecture and proper amount of training samples (20k).

2) Comparison with baseline methods on the VoxCeleb2:

Table II reports the performance of SEANet and baseline methods on the VoxCeleb2 dataset. Our SEANet performs the best SI-SDR and SDR on the VoxCeleb2, for instance, 12.88 dB SI-SDR from SEANet vs 10.84 SI-SDR from AV-Sep. Also, SEANet achieves the best PESQ and STOI with 2.34 and 0.89, respectively. Noted that the PESQ in VoxCeleb2 is slightly better than that in LRS2 because the videos in VoxCeleb2 have the longer duration. In summary, SEANet achieves an obvious improvement over the previous methods for all eight metrics. Considering that VoxCeleb2 contains the many noisy videos, these results verify that SEANet can handle the AV-TSE task well for the challenging dataset by analysing the noise intelligently.

3) **Comparison with other methods on the LRS2 or VoxCeleb2:** Besides the three baseline methods, some other AV-TSE solutions are studied in previous works. Here, we compare SEANet with them from the corresponding published paper in Table III. We summarise the results in SI-SDR and SDR since most of these works focus on these two metrics. Note that the experimental settings and trial selections are slightly different in these works. So we remark the number of training data in Table III. Compared with the best previous works for the VoxCeleb2 dataset (12.13 dB from AV-Sepformer), SEANet uses fewer or equal samples for training

TABLE I

COMPARISON OF SEANet AND BASELINE METHODS FOR NINE EVALUATION METRICS, WE TRAIN AND EVALUATE THEM ON THE LRS2 DATASET WITH THE SAME SETTING. NOTE THAT ALL RESULTS COME FROM OUR OWN RE-IMPLEMENT FOR FAIR COMPARISON. LOWER IS BETTER FOR WER AND HIGHER IS BETTER FOR THE REST METRICS.

Method	# Param	Metrics								
		SI-SDR	SDR	PESQ	STOI	SI-SDRi	SDRi	PESQi	STOii	WER (%)
AV-DPRNN	4.12M	10.24	10.81	1.88	0.88	10.29	10.65	0.70	0.22	14.81
MuSE [5]	15.01M	10.97	11.57	1.98	0.90	11.01	11.41	0.80	0.24	13.56
AV-Sep [6]	21.73M	12.60	13.13	2.20	0.91	12.64	12.97	1.02	0.26	12.82
SEANet	8.70M	13.08	13.67	2.25	0.92	13.05	13.52	1.07	0.29	12.26

TABLE II

COMPARISON OF SEANet AND BASELINE METHODS FOR EIGHT EVALUATION METRICS, WE TRAIN AND EVALUATE THEM ON THE VOXCELEB2 DATASET WITH THE SAME SETTING. NOTE THAT ALL RESULTS COME FROM OUR OWN RE-IMPLEMENT FOR FAIR COMPARISON. HIGHER IS BETTER FOR ALL THESE METRICS.

Method	# Param	Metrics							
		SI-SDR	SDR	PESQ	STOI	SI-SDRi	SDRi	PESQi	STOii
AV-DPRNN	4.12M	11.13	11.55	2.09	0.86	11.02	11.35	0.84	0.23
MuSE [5]	15.01M	10.89	11.34	2.11	0.86	10.78	10.51	0.86	0.23
AV-Sep [6]	21.73M	12.07	12.49	2.25	0.88	11.96	12.29	1.00	0.24
SEANet	8.70M	12.88	13.33	2.34	0.89	12.77	13.13	1.09	0.25

and achieves 0.75 dB SI-SDR improvement. Similarly, for the LRS2 dataset, SEANet achieves 1.88 dB SI-SDR improvement compared to the previous method (11.3dB from Conversation). That guarantees our study’s rigour.

TABLE III

COMPARISON OF SEANet AND PREVIOUS METHODS ON THE LRS2 DATASET OR VOXCELEB2 DATASET. THESE RESULTS COME FROM THEIR ORIGINAL PAPER. † DENOTES THAT VALUE IS SDRi. ‘-’ MEANS THAT NUMBER IS NOT REPORTED IN THE ORIGINAL PAPER.

Dataset	Method	SI-SDR	SDR	# training data
LRS2	CaffNet-C [56]	10.01	-	-
	LWTNet [57]	10.80	-	-
	Conversation [4]	11.30	-	-
	SEANet	13.08	13.67	20k
VoxCeleb2	Face filter [58]	-	2.53†	200k
	Conversation [4]	-	7.90	-
	VisualVoice [19]	9.73	10.20	> 1,000k
	AV-Conv [14]	10.38	10.90†	40k
	MuSE [5], [6]	11.24	-	20k
	AVDiffuSS [59]	12.03	-	> 1,000k
	AV-Sep [6]	12.13	-	20k
	SEANet	12.88	13.33	20k

B. Cross-domain evaluation: LRS3, Grid and TCD-TIMIT

Then, we conduct the cross-domain evaluation for SEANet and the baseline methods on Table IV based on SI-SDR, SDR, PESQ and STOI. The evaluation sets are LRS3, Grid and TCD-TIMIT datasets. We find that the videos in the Grid dataset are not strictly synchronized. However, all videos in the LRS2 dataset are strictly synchronized. This setting mismatch can lead to a performance gap. Due to that, all methods are trained on the VoxCeleb2 for fair comparison.

For the results on LRS3 and Grid, SEANet performs better than all baseline methods for all evaluation metrics. In the TCD-TIMIT dataset, AV-Sepformer performs slightly better than SEANet for two metrics. However, compared with AV-Sepformer, SEANet only used around 40% number of model parameters. So extending the model size of SEANet can achieve better performance. In summary, the average SI-SDR and PESQ of SEANet for three datasets are over 13.81 dB and

2.42, which represents a good extraction quality. Considering the diversity of these evaluation sets, these experiments prove the robustness of our proposed SEANet and the value of exploring noise signals.

TABLE IV

CROSS-DOMAIN EVALUATION OF SEANet AND THE BASELINE METHODS, ALL METHODS ARE TRAINED ON VOXCELEB2, THEN TEST ON LRS3, GRID AND TCD-TIMIT DATASETS. HIGHER IS BETTER FOR ALL THESE METRICS.

Evaluation Sets	Method	Metrics			
		SI-SDR	SDR	PESQ	STOI
LRS3	AV-DPRNN	12.83	13.31	2.17	0.92
	MuSE [5]	12.58	13.08	2.15	0.92
	AV-Sep [6]	14.52	14.96	2.40	0.93
	SEANet	14.75	15.23	2.42	0.93
TCD	AV-DPRNN	12.24	13.14	2.32	0.88
	MuSE [5]	12.57	13.25	2.33	0.89
	AV-Sep [6]	14.15	14.81	2.49	0.91
	SEANet	14.10	15.02	2.44	0.91
Grid	AV-DPRNN	11.59	12.58	2.24	0.87
	MuSE [5]	11.19	12.19	2.27	0.88
	AV-Sep [6]	12.20	13.20	2.32	0.88
	SEANet	12.59	14.45	2.43	0.88

C. Ablation study for efficiency

This section conducts the ablation studies to prove the efficiency of SEANet architecture and analyse why SEANet can achieve better performance. Here, we consider AV-DPRNN for comparison since it shares the similar model architecture with our SEANet, the difference is that SEANet involves reverse attention to learn the speech-noise interaction. As we mentioned, some videos in VoxCeleb2 are out of sync by -0.08 to 0.08 seconds. Our ablation studies are conducted on the LRS2 dataset.

1) **Reverse attention:** To verify that the proposed reverse selective auditory attention ability is important to assist the extraction process, we consider the following structures in Figure 7 for comparison: AV-DPRNN has the speech branch only. S1 contains the speech-speech interaction with attention (Eq. 2 contains self-attention A_{s+} only). S2 has the noisy

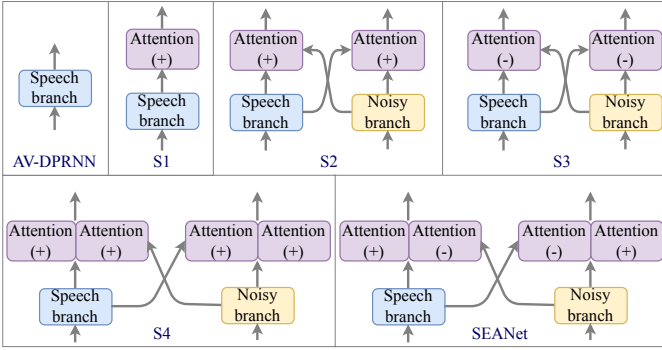


Fig. 7. Four kinds of architecture for ablation study. Attention (+) denotes the normal self-attention, Attention (-) denotes the proposed reverse attention. S1 involves the self-attention for speech branch; S2 contains the positive cross-attention for speech-noise interaction; similar to S2, S4 adds the self-attention in both speech branch and noisy branch. S3 contains the reverse attention for speech branch and noisy branch.

branch, the speech-noise interaction is conducted based on traditional self-attention (Eq. 2 contains A_{s-} only without reverse operation). S3 is similar to S2, while speech-noise interaction based on reverse attention (Eq. 2 contains A_{s-} only). S4 has speech-noise and speech-speech interaction attention, both of them apply traditional self-attention (A_{s-} in Eq. 2 has no reverse operation). SEANet contains the reverse attention for speech-noise interaction and self-attention for speech-speech interaction.

We train these structures with the same setting and summarize the results in Table V: 1) Speech-speech attention can assist AV-TSE by learning voice consistency (AV-DPRNN vs S1). 2) The noisy branch can help the AV-TSE training by understanding the speech-noise interaction (AV-DPRNN vs S2 and S3). 3) Moreover, reverse attention performs slightly better than traditional self-attention in studying speech-noise interaction (S2 vs S3, S4 vs SEANet). 4) SEANet can achieve the best performance by incorporating reverse attention and self-attention.

TABLE V

ABLATION STUDY FOR THE DIFFERENT NETWORK STRUCTURES. \oplus DENOTE TYPICAL SELF-ATTENTION, WHICH IS POSITIVE; \ominus REPRESENTS OUR PROPOSED REVERSE ATTENTION, WHICH IS NEGATIVE. EXPERIMENTS ARE CONDUCTED ON THE LRS2 DATASET. ILLUSTRATIONS OF THESE STRUCTURES CAN BE FOUND IN FIG 7

Method	Speech-noise attention	Speech-speech attention	SI-SDR	SDR
AV-DPRNN	\times	\times	10.24	10.81
S1	\times	\oplus	12.18	12.79
S2	\oplus	\times	12.51	13.05
S3	\ominus	\times	12.71	13.33
S4	\oplus	\oplus	12.75	13.39
SEANet	\ominus	\oplus	13.08	13.67

2) **Model size:** As we mentioned, SEANet can perform better than MuSE and AV-Sepformer with the smaller model size: 8.70M (SEANet) vs 15.01M (MuSE) and 21.73M (AV-Sepformer). Considering that SEANet has more number parameters than the AV-DPRNN, which shares a similar RNN-based architecture except involving the noisy branch, Table VI propose two new structures to study the efficiency of SEANet

further. ‘-deeper’ means AV-DPRNN with more layers (R) and ‘-wider’ represents AV-DPRNN with the larger feature dimension (D). These two systems have more parameters than SEANet, while from the results on LRS2, SEANet still achieves better SI-SDR and SDR with over 1.5 dB difference. These experiments prove that our improvement is not parameters-driven.

TABLE VI

ABLATION STUDY FOR THE MODEL SIZE, SEANet CAN PERFORM BETTER THAN THE DEEPER OR LARGER AV-DPRNN WITH THE SMALLER ARCHITECTURE.

Method	# Param	SI-SDR	SDR	Setting
AV-DPRNN	4.12M	10.24	10.81	$R = 6, D = 64$
-deeper	9.32M	11.25	11.80	$R = 15, D = 64$
-wider	11.88M	11.45	12.01	$R = 6, D = 128$
SEANet	8.70M	13.08	13.67	$R = 6, D = 64$

3) **Extraction correctness:** Then, we study whether SEANet obtains the improvement by achieving more correct extraction. During the evaluation, we split the speech into segments of fixed duration T . Consider $l(\hat{s}, s)$ as the SI-SDR between the estimated speech \hat{s} and the ground-truth speech s . We define that the extraction in one audio segment is incorrect if the extracted audio is much close to the ground-truth noise n instead of the ground-truth speech s : $l(\hat{s}, s) < l(\hat{s}, n) - \mu$. Here, we involve μ as the threshold where Lower T and higher μ will lead to more stringent requirements and incorrect extraction segments. Figure 8 shows the total number of incorrect extraction segments during the evaluation. Compared with the results of AV-DPRNN on the left side, SEANet leads to less incorrect extraction for all the settings. That verifies our assumption that SEANet can alleviate incorrect speaker extraction to improve performance.

(a) AV-DPRNN					(b) SEANet				
threshold μ (dB)	1	0.8	0.6	0.4	1	0.8	0.6	0.4	
0	5	7	31	71	3	3	10	27	
2	8	12	42	101	5	3	12	33	
4	12	20	63	138	6	7	15	42	
6	19	27	75	180	8	12	17	59	
8	34	37	96	233	11	14	20	81	
10	48	50	122	303	14	16	33	112	

Fig. 8. The total number of INCORRECT speaker extraction segments during evaluation. Larger number represents more incorrect extractions.

D. Quality study for robustness

In this section, we conduct quality studies to learn the robustness of the proposed SEANet under the different training or evaluation settings. Similarly, we evaluate the AV-DPRNN system for comparison on the LRS2 dataset.

1) **Hyper-parameter:** Figure 10 studies the robustness of SEANet when training with the different hyper-parameter β in the loss function Eq. 7. Note that SEANet degrades to AV-DPRNN when β is equal to zero. From this figure, SEANet is

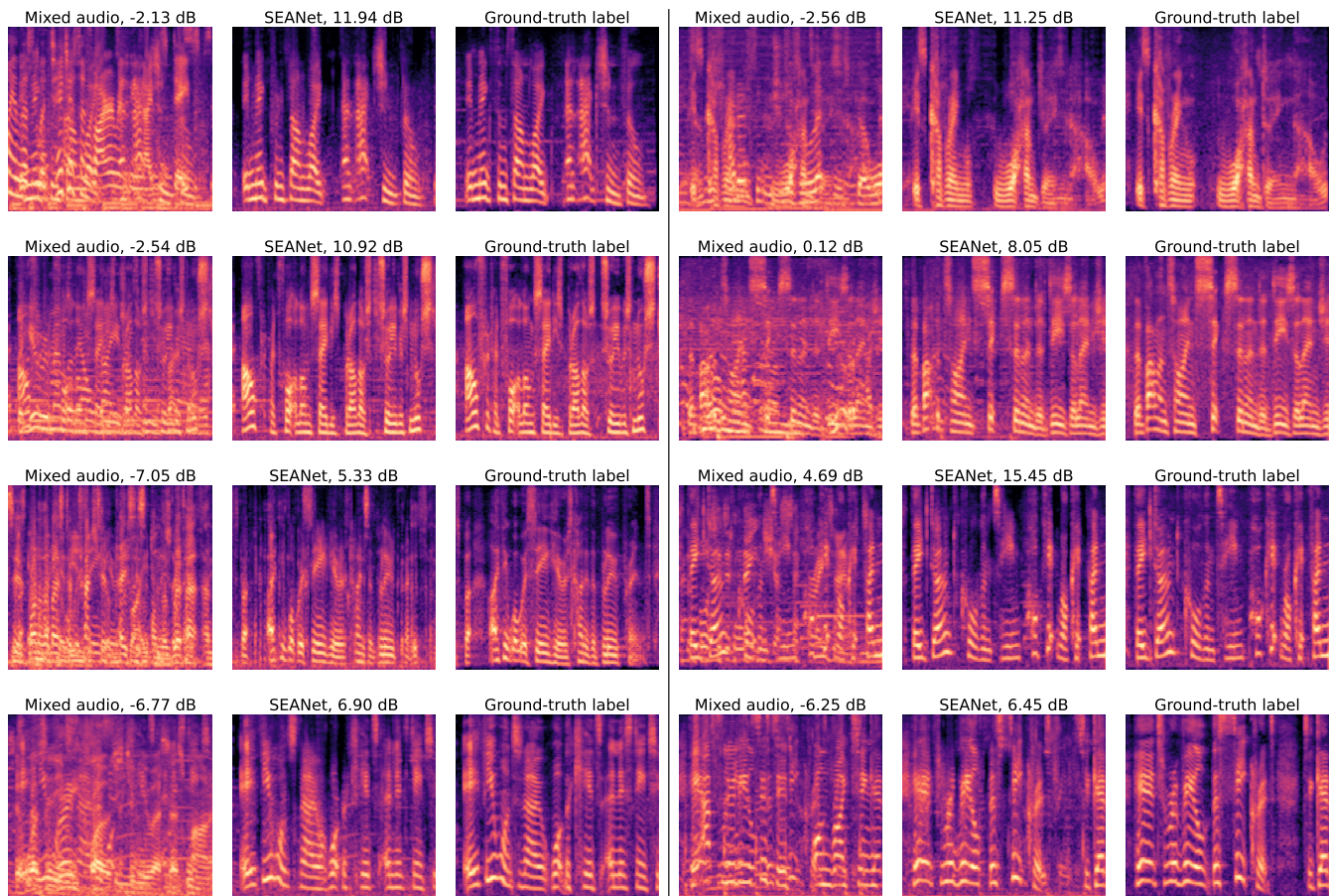


Fig. 9. SEANet extraction visualization for 8 samples in the LRS2 with SI-SDR. Each figure represents the Mel spectrogram of the mixed audio and the SEANet’s output speech. The corresponding SI-SDR is also provided. Compared with the mixed audio, SEANet is able to filter the noise and improve the SI-SDR.

stable under the different β over zero. A lower value of β can lead to better performance, and SEANet can achieve the best performance when β equals 0.1. That proves our SEANet is not sensitive to the hyper-parameter selection.

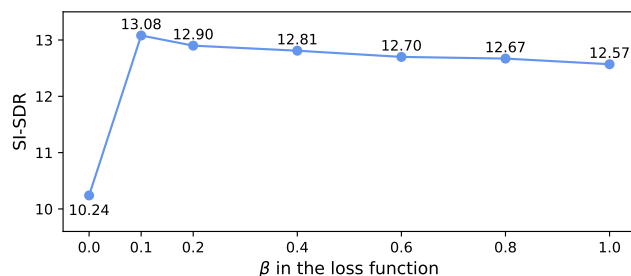


Fig. 10. Study for the effect of hyper-parameter β in the loss function for SEANet. SEANet degrades to baseline AV-DPRNN when $\beta = 0$.

2) *AV-TSE for ordinary acoustic environment*: Then, we report the results of SEANet for ordinary acoustic environment: when the mixture of audio contains the speech from the target speaker and the non-speech noise only, our task can be viewed as audio-visual speech enhancement. We train the AV-DPRNN and SEANet based on these speech enhancement

format data for comparison. In Table VII, we report the results with the different Signal-to-Noise Ratio (SNR) for the input audio. SEANet performs better than AV-DPRNN for this enhancement task under different noise levels with the very stable improvement. Meanwhile, a very high SI-SDR can be achieved in this enhancement task. Because extracting the target speaker’s speech from the non-speech noise is easier than extracting it from the mixture of speech.

Method	Input SNR (dB)	SI-SDR	SDR	SI-SDR _i	SDR _i
AV-DPRNN	5	13.86	14.42	8.75	9.23
	10	16.96	17.51	6.85	7.34
	15	19.68	20.31	4.57	5.14
	20	21.77	22.57	1.66	2.40
SEANet	5	14.67	15.23	9.57	10.04
	10	17.67	18.21	7.57	8.03
	15	20.39	20.99	5.29	5.82
	20	22.36	23.06	2.25	2.88

TABLE VII
PERFORMANCE OF AV-DPRNN AND THE PROPOSED SEANET IN THE ORDINARY ACOUSTIC ENVIRONMENT FOR AUDIO-VISUAL SPEECH ENHANCEMENT TASK. THE INPUT AUDIO CONTAINS THE TARGET SPEAKER’S SPEECH AND THE NON-SPEECH NOISE. INPUT SNR (dB) INDICATES THE SNR FOR THE INPUT AUDIO TO REPRESENT THE DIFFERENT NOISY LEVEL.

3) *AV-TSE for challenging acoustic environments*: Our previous results have shown that SEANet can handle the sce-

nario of two speakers talking simultaneously. Here, we further study the robustness of our SEANet in challenging acoustic environments. As shown in Table VIII, the audio mixture contains the target speaker’s speech. Then, ‘S’ denotes the existence of one interference speaker. ‘N’ means the existence of non-speech noise, such as background noise or music. For instance, ‘S + S + N’ represents the input audio containing the target speaker’s voice, two other speakers’ voices and the non-speech noise. This can simulate very complex extraction conditions.

In this experiment, instead of training with the mixed audio of two speakers’ voices only, both AV-DPRNN and SEANet are trained with the data from these four scenarios to boost the application ability. From the results, a more noisy environment leads to a low SI-SDR and SDR since the extraction becomes challenging. At the same time, the SI-SDR_i and SDR_i are relatively stable. Compared with AV-DPRNN, SEANet shows more excellent stability under all conditions. In these challenge scenarios, it consistently achieves impressive SISDR, SDR, SISDR_i, and SDR_i.

Method	Interference	SI-SDR	SDR	SI-SDR _i	SDR _i
AV-DPRNN	S	10.44	11.13	10.49	10.97
	S + N	8.93	9.64	9.86	10.36
	S + S	5.48	6.35	9.95	10.50
	S + S + N	4.93	5.82	9.71	10.27
SEANet	S	13.21	14.05	13.26	13.89
	S + N	11.37	12.21	12.31	12.94
	S + S	7.94	8.89	12.41	13.04
	S + S + N	7.20	8.16	11.98	12.60

TABLE VIII

PERFORMANCE OF AV-DPRNN AND THE PROPOSED SEANET IN THE CHALLENGING ACOUSTIC ENVIRONMENT. FOR THE MIXTURE OF AUDIO WHICH CONTAINS THE TARGET SPEAKER’S SPEECH, ‘S’ DENOTES THE EXISTENCE OF ONE INTERFERENCE SPEAKER, AND ‘N’ DENOTES THE EXISTENCE OF THE NON-SPEECH NOISY SIGNAL.

E. Visualization

In this section, we provide some visualization results of SEANet. These results are also achieved on the LRS2 dataset.

1) **Extraction visualization:** Figure 9 visualizes the extraction results of eight random audio samples. Each line contains two samples. For each sample, we provide the Mel spectrogram of the mixed audio, the SEANet’s output speech and the ground truth speech for comparison. The SI-SDR for the mixed audio and the output speech has also been provided. Compared with the mixed audio, the output speech resembles the ground-truth speech. These visualization results demonstrate that SEANet can achieve robust extraction in both easy (high original SI-SDR) and challenging (low original SI-SDR) scenarios.

2) **Attention score visualization:** Figure 11 indicates the attention visualization for A_s in Eq. 2. There are ten attention maps since SEANet contains $R = 5$ PSNL blocks with intra-chunk and inter-chunk attention. Intra-chunk attention is used in each chunk to search the local information, it focuses on the diagonals frame-wise correlation. Inter-chunk attention works across all chunks to learn the global correlation, it focuses on the knowledge within rows and columns. The deeper layer learns more representative information. Each attention score

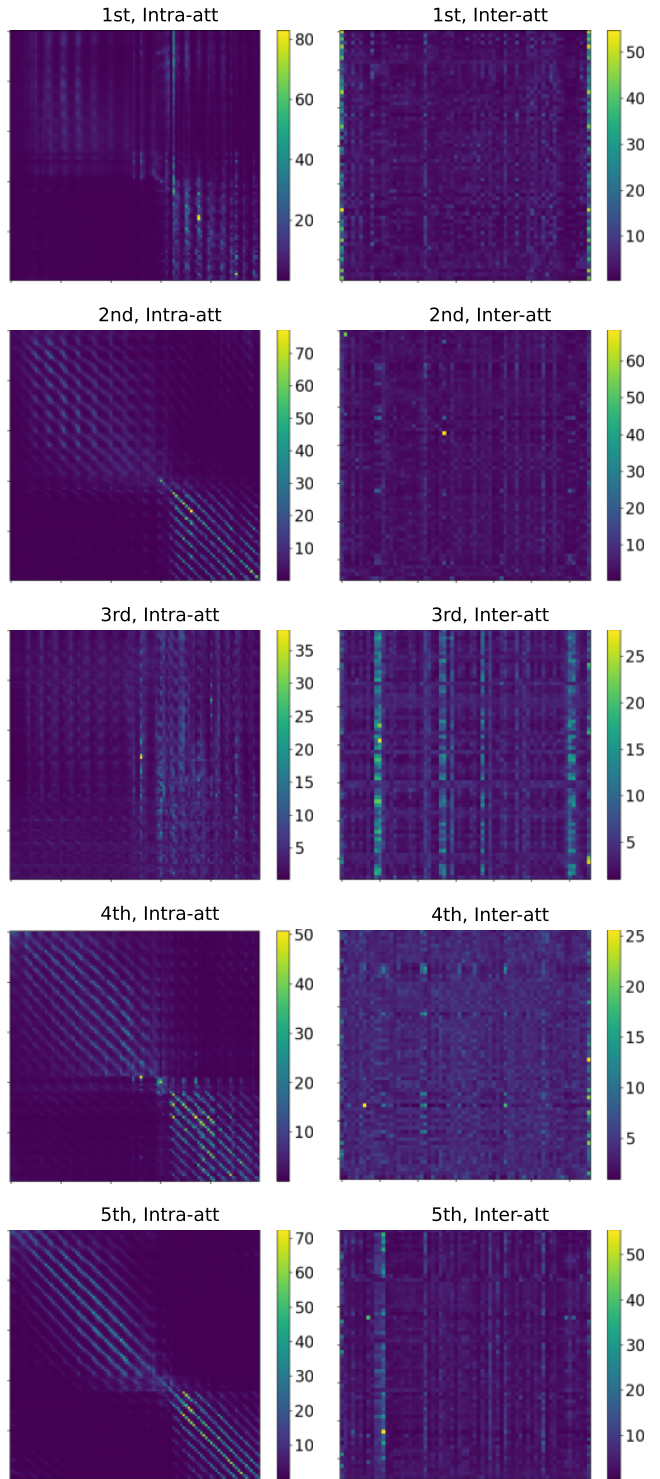


Fig. 11. Visualization for the attention score matrix A_s in each PSNL block, the left and right column represents the intra-chunk and inter-chunk attention, respectively. The attention map for intra-chunk correlation focuses on the diagonals. In contrast, the attention map for inter-chunk correlation concentrates on the rows and columns.

contains the self-attention part to study the voice consistency and the reverse attention to exclude the noisy signals.

VI. DISCUSSION

We further discuss the problems we found in the experimental process and provide our analysis.

A. Extraction vs separation

For audio-visual target speaker extraction (AV-TSE) [4], [5] and audio-visual speech separation [60]. Although both require information from face frames, 1) the separation model needs the face from multiple sound sources. In contrast, AV-TSE requires the target face only, which is a more convenient solution. 2) during training and testing, the separation model requires the same number of speakers due to the fixed model structure, while the extraction model can handle any number of speakers by applying the model multiple times. In summary, AV-TSE is a more feasible direction for diverse real-world conversations.

B. Video quality for AV-TSE

We find that the audio in VoxCeleb2 is not clean enough because it is collected from the interviewers with background music, noise, or even other speakers' speech. Therefore, using such speech as the flawed ground-truth label will damage many extraction systems since we usually assume the ground-truth label is absolutely correct. Furthermore, VoxCeleb2 has many out-of-sync videos, while AV-TSE models are designed based on the strictly synchronized condition. Previous study [56] has verified that the audio-visual offset will affect AV-TSE. It is important to analyze the advantages and disadvantages of using such an imperfect dataset for AV-TSE. Meanwhile, studying the extraction under challenging real-world conditions, such as discontinuous face frames and the boisterous environment, is also meaningful.

VII. CONCLUSION

In this paper, we propose the Subtraction-and-ExtrAction network (SEANet) for audio-visual target speaker extraction (AV-TSE). SEANet focuses on reverse selective auditory attention to force the neural network to understand the noisy signal during extraction. Our experimental results verify that this 'subtraction' strategy can suppress noisy signal and avoid incorrect speaker extraction. SEANet outperforms previous methods for five different datasets under up to nine metrics. In future work, we will extend the reverse selective auditory attention mechanism to the audio-only target speaker extraction. Furthermore, we will analyse the roles of each auxiliary reference to achieve an intelligent balance between them.

REFERENCES

- [1] E. C. Cherry, "Some experiments on the recognition of speech, with one and with two ears," *The Journal of the acoustical society of America*, vol. 25, no. 5, pp. 975–979, 1953.
- [2] E. Z. Golombic, G. B. Cogan, C. E. Schroeder, and D. Poeppel, "Visual input enhances selective speech envelope tracking in auditory cortex at a "cocktail party"," *Journal of Neuroscience*, vol. 33, no. 4, pp. 1417–1426, 2013.
- [3] R. Cutler and L. Davis, "Look who's talking: Speaker detection using video and audio correlation," in *Int. Conf. Multimedia and Expo*, vol. 3. IEEE, 2000, pp. 1589–1592.
- [4] T. Afouras, J. S. Chung, and A. Zisserman, "The Conversation: deep audio-visual speech enhancement," *Interspeech*, pp. 3244–3248, 2018.
- [5] Z. Pan, R. Tao, C. Xu, and H. Li, "Muse: Multi-modal target speaker extraction with visual cues," in *ICASSP*. IEEE, 2021, pp. 6678–6682.
- [6] J. Lin, X. Cai, H. Dinkel, J. Chen, Z. Yan, Y. Wang, J. Zhang, Z. Wu, Y. Wang, and H. Meng, "Av-sepformer: Cross-attention sepformer for audio-visual target speaker extraction," in *ICASSP*. IEEE, 2023.
- [7] J. Wang, X. Qian, and H. Li, "Predict-and-update network: Audio-visual speech recognition inspired by human speech perception," *arXiv preprint arXiv:2209.01768*, 2022.
- [8] B. Shi, W.-N. Hsu, K. Lakhota, and A. Mohamed, "Learning audio-visual speech representation by masked multimodal cluster prediction," *arXiv preprint arXiv:2201.02184*, 2022.
- [9] M. Cheng and M. Li, "Multi-input multi-output target-speaker voice activity detection for unified, flexible, and robust audio-visual speaker diarization," *arXiv preprint arXiv:2401.08052*, 2024.
- [10] R. Tao, Z. Pan, R. K. Das, X. Qian, M. Z. Shou, and H. Li, "Is someone speaking? exploring long-term temporal features for audio-visual active speaker detection," in *ACM Int. Conf. Multimedia*, 2021, p. 3927–3935.
- [11] R. Tao, K. A. Lee, R. K. Das, V. Hautamäki, and H. Li, "Self-supervised training of speaker encoder with multi-modal diverse positive pairs," *IEEE Trans. on Audio, Speech, and Language Processing*, 2023.
- [12] D. Cai, W. Wang, and M. Li, "Incorporating visual information in audio based self-supervised speaker recognition," *IEEE Trans. on Audio, Speech, and Language Processing*, 2022.
- [13] M. Dianatfar, J. Latokartano, and M. Lanz, "Review on existing vr/ar solutions in human–robot collaboration," *Procedia CIRP*, vol. 97, pp. 407–411, 2021.
- [14] J. Wu, Y. Xu, S.-X. Zhang, L.-W. Chen, M. Yu, L. Xie, and D. Yu, "Time domain audio visual speech separation," in *IEEE Automatic Speech Recognition and Understanding Workshop*. IEEE, 2019, pp. 667–673.
- [15] J. Li, M. Ge, Z. Pan, R. Cao, L. Wang, J. Dang, and S. Zhang, "Rethinking the Visual Cues in Audio-Visual Speaker Extraction," in *Interspeech*, 2023, pp. 3754–3758.
- [16] G. M. Edelman, *Neural Darwinism: The theory of neuronal group selection*. Basic books, 1987.
- [17] M. J. Crosse, G. M. Di Liberto, and E. C. Lalor, "Eye can hear clearly now: inverse effectiveness in natural audiovisual speech processing relies on long-term crossmodal temporal integration," *Journal of Neuroscience*, vol. 36, no. 38, pp. 9888–9895, 2016.
- [18] H. L. Bear and R. Harvey, "Phoneme-to-viseme mappings: the good, the bad, and the ugly," *Speech Communication*, vol. 95, pp. 40–67, 2017.
- [19] R. Gao and K. Grauman, "Visualvoice: Audio-visual speech separation with cross-modal consistency," in *IEEE Conf. Comput. Vis. Pattern Recog.* IEEE, 2021, pp. 15 490–15 500.
- [20] K. Li, R. Yang, and X. Hu, "An efficient encoder-decoder architecture with top-down attention for speech separation," in *The Eleventh International Conference on Learning Representations*, 2023.
- [21] Y. Luo and N. Mesgarani, "Conv-TasNet: Surpassing ideal time-frequency magnitude masking for speech separation," *IEEE Trans. on Audio, Speech, and Language Processing*, vol. 27, no. 8, pp. 1256–1266, 2019.
- [22] Z. Pan, R. Tao, C. Xu, and H. Li, "Selective listening by synchronizing speech with lips," *IEEE Trans. on Audio, Speech, and Language Processing*, vol. 30, pp. 1650–1664, 2022.
- [23] A. Vaswani, N. Shazeer, N. Parmar, J. Uszkoreit, L. Jones, A. N. Gomez, E. Kaiser, and I. Polosukhin, "Attention is all you need," *Advances in neural information processing systems*, vol. 30, 2017.
- [24] Y. Luo, Z. Chen, and T. Yoshioka, "Dual-path rnn: efficient long sequence modeling for time-domain single-channel speech separation," in *ICASSP*. IEEE, 2020, pp. 46–50.
- [25] Z. Pan, M. Ge, and H. Li, "Usev: Universal speaker extraction with visual cue," *IEEE Trans. on Audio, Speech, and Language Processing*, vol. 30, pp. 3032–3045, 2022.
- [26] Z. Zhao, D. Yang, R. Gu, H. Zhang, and Y. Zou, "Target confusion in end-to-end speaker extraction: Analysis and approaches," *Interspeech*, 2022.
- [27] S. Chen, X. Tan, B. Wang, and X. Hu, "Reverse attention for salient object detection," in *Eur. Conf. Comput. Vis.*, 2018, pp. 234–250.
- [28] C. Zheng, X. Peng, Y. Zhang, S. Srinivasan, and Y. Lu, "Interactive speech and noise modeling for speech enhancement," in *AAAI*, vol. 35, 2021, pp. 14 549–14 557.
- [29] Y. Hu, N. Hou, C. Chen, and E. S. Chng, "Interactive feature fusion for end-to-end noise-robust speech recognition," in *ICASSP*. IEEE, 2022, pp. 6292–6296.

- [30] Q. Wang, H. Muckenhirn, K. Wilson, P. Sridhar, Z. Wu, J. Hershey, R. A. Saurous, R. J. Weiss, Y. Jia, and I. L. Moreno, "Voicefilter: Targeted voice separation by speaker-conditioned spectrogram masking," *Interspeech*, 2019.
- [31] M. Delcroix, K. Zmolikova, K. Kinoshita, A. Ogawa, and T. Nakatani, "Single channel target speaker extraction and recognition with speaker beam," in *ICASSP*. IEEE, 2018, pp. 5554–5558.
- [32] D. Wang and J. Chen, "Supervised speech separation based on deep learning: An overview," *IEEE Trans. on Audio, Speech, and Language Processing*, vol. 26, no. 10, pp. 1702–1726, 2018.
- [33] C. Subakan, M. Ravanelli, S. Cornell, M. Bronzi, and J. Zhong, "Attention is all you need in speech separation," in *ICASSP*. IEEE, 2021, pp. 21–25.
- [34] D. Yu, M. Kolbæk, Z.-H. Tan, and J. Jensen, "Permutation invariant training of deep models for speaker-independent multi-talker speech separation," in *ICASSP*. IEEE, 2017, pp. 241–245.
- [35] C. Xu, W. Rao, E. S. Chng, and H. Li, "Time-domain speaker extraction network," in *2019 IEEE Automatic Speech Recognition and Understanding Workshop (ASRU)*. IEEE, 2019, pp. 327–334.
- [36] —, "Spex: Multi-scale time domain speaker extraction network," *IEEE Trans. on Audio, Speech, and Language Processing*, vol. 28, pp. 1370–1384, 2020.
- [37] M. Ge, C. Xu, L. Wang, E. S. Chng, J. Dang, and H. Li, "Spex+: A complete time domain speaker extraction network," *Interspeech*, 2020.
- [38] N. Dehak, P. J. Kenny, R. Dehak, P. Dumouchel, and P. Ouellet, "Front-end factor analysis for speaker verification," *IEEE Trans. on Audio, Speech, and Language Processing*, vol. 19, no. 4, pp. 788–798, 2010.
- [39] D. Snyder, P. Ghahremani, D. Povey, D. Garcia-Romero, Y. Carmiel, and S. Khudanpur, "Deep neural network-based speaker embeddings for end-to-end speaker verification," in *IEEE Spoken Language Technology Workshop (SLT)*. IEEE, 2016, pp. 165–170.
- [40] L. Wan, Q. Wang, A. Papir, and I. L. Moreno, "Generalized end-to-end loss for speaker verification," in *ICASSP*. IEEE, 2018, pp. 4879–4883.
- [41] Z. Mu, X. Yang, S. Sun, and Q. Yang, "Self-supervised disentangled representation learning for robust target speech extraction," in *Proceedings of the AAAI Conference on Artificial Intelligence*, vol. 38, no. 17, 2024, pp. 18 815–18 823.
- [42] Z. Zhang, B. He, and Z. Zhang, "X-tasnet: Robust and accurate time-domain speaker extraction network," in *Interspeech*, 2020, pp. 1421–1425.
- [43] M. Ge, C. Xu, L. Wang, E. S. Chng, J. Dang, and H. Li, "L-spex: Localized target speaker extraction," in *ICASSP*. IEEE, 2022, pp. 7287–7291.
- [44] H. Sato, T. Ochiai, K. Kinoshita, M. Delcroix, T. Nakatani, and S. Araki, "Multimodal attention fusion for target speaker extraction," in *IEEE Spoken Language Technology Workshop (SLT)*. IEEE, 2021, pp. 778–784.
- [45] H. Lin, Y. Zhuang, Y. Huang, X. Ding, X. Liu, and Y. Yu, "Noise2grad: Extract image noise to denoise," in *IJCAI*, 2021, pp. 830–836.
- [46] D.-P. Fan, G.-P. Ji, T. Zhou, G. Chen, H. Fu, J. Shen, and L. Shao, "Pranet: Parallel reverse attention network for polyp segmentation," in *International conference on medical image computing and computer-assisted intervention*. Springer, 2020, pp. 263–273.
- [47] T. Afouras, J. S. Chung, A. Senior, O. Vinyals, and A. Zisserman, "Deep audio-visual speech recognition," *IEEE Trans. Pattern Anal. Mach. Intell.*, 2018.
- [48] J. Le Roux, S. Wisdom, H. Erdogan, and J. R. Hershey, "SDR–half-baked or well done?" in *ICASSP*. IEEE, 2019, pp. 626–630.
- [49] J. S. Chung, A. Nagrani, and A. Zisserman, "VoxCeleb2: Deep speaker recognition," in *Interspeech*, 2018, pp. 1086–1090.
- [50] T. Afouras, J. S. Chung, and A. Zisserman, "LRS3-TED: a large-scale dataset for visual speech recognition," *arXiv preprint arXiv:1809.00496*, 2018.
- [51] N. Alghamdi, S. Maddock, R. Marxer, J. Barker, and G. J. Brown, "A corpus of audio-visual lombard speech with frontal and profile views," *The Journal of the Acoustical Society of America*, vol. 143, no. 6, pp. EL523–EL529, 2018.
- [52] N. Harte and E. Gillen, "TCD-TIMIT: An audio-visual corpus of continuous speech," *IEEE Trans. Multimedia*, vol. 17, no. 5, pp. 603–615, 2015.
- [53] A. W. Rix, J. G. Beerends, M. P. Hollier, and A. P. Hekstra, "Perceptual evaluation of speech quality (PESQ)-a new method for speech quality assessment of telephone networks and codecs," in *ICASSP*, vol. 2. IEEE, 2001, pp. 749–752.
- [54] C. H. Taal, R. C. Hendriks, R. Heusdens, and J. Jensen, "A short-time objective intelligibility measure for time-frequency weighted noisy speech," in *ICASSP*. IEEE, 2010, pp. 4214–4217.
- [55] A. Radford, J. W. Kim, T. Xu, G. Brockman, C. McLeavey, and I. Sutskever, "Robust speech recognition via large-scale weak supervision," in *International Conference on Machine Learning*, 2023, pp. 28 492–28 518.
- [56] J. Lee, S.-W. Chung, S. Kim, H.-G. Kang, and K. Sohn, "Looking into your speech: Learning cross-modal affinity for audio-visual speech separation," in *Proceedings of the IEEE/CVF Conference on Computer Vision and Pattern Recognition*, 2021, pp. 1336–1345.
- [57] T. Afouras, A. Owens, J. S. Chung, and A. Zisserman, "Self-supervised learning of audio-visual objects from video," in *Eur. Conf. Comput. Vis.*, 2020.
- [58] S. W. Chung, S. Choe, J. S. Chung, and H. G. Kang, "Facefilter: Audio-visual speech separation using still images," in *Proceedings of the Annual Conference of the International Speech Communication Association, INTERSPEECH*, vol. 2020, 2020, pp. 3481–3485.
- [59] S. Lee, C. Jung, Y. Jang, J. Kim, and J. S. Chung, "Seeing through the conversation: Audio-visual speech separation based on diffusion model," *arXiv preprint arXiv:2310.19581*, 2023.
- [60] A. Ephrat, I. Mosseri, O. Lang, T. Dekel, K. Wilson, A. Hassidim, W. T. Freeman, and M. Rubinstein, "Looking to listen at the cocktail party: A speaker-independent audio-visual model for speech separation," *ACM Transactions on Graphics*, vol. 37, no. 4, pp. 112:1–112:11, 2018.